SCIENTIFIC REPORTS

OPEN

SUBJECT AREAS:
GENE EXPRESSION
SKIN STEM CELLS

Received
20 August 2014

Accepted
19 December 2014

Published
21 January 2015

Correspondence and requests for materials should be addressed to S.L. (liushuang@ioz.ac.cn) or E.D. (duane@ioz.ac.cn)

GPR39 marks specific cells within the sebaceous gland and contributes to skin wound healing

Huashan Zhao[1,2], Jingqiao Qiao[3], Shoubing Zhang[4], Huishan Zhang[1], Xiaohua Lei[1], Xinyue Wang[1], Zhili Deng[1,2], Lina Ning[1], Yujing Cao[1], Yong Guo[3], Shuang Liu[1] & Enkui Duan[1]

[1]State Key Laboratory of Reproductive Biology, Institute of Zoology, Chinese Academy of Sciences, Beijing, China, [2]University of Chinese Academy of Sciences, Beijing, China, [3]College of Animal Science and Technology, Beijing University of Agriculture, China, [4]Department of Histology&Embryology, School of Basic Medical Sciences, Anhui Medical University, Hefei, China.

G protein-coupled receptors (GPCRs) mediate multiple key biological processes in the body. The orphan receptor GPR39 has been reported to be involved in various pathophysiological events. However, the function of GPR39 in skin biology remains unknown. Using a genetically engineered mouse strain in which *lacZ* expression faithfully replaced endogenous *Gpr39* expression, we discovered a unique expression pattern of *Gpr39* in the sebaceous gland (SG). Using various methods, we confirmed that GPR39 marked a specific cell population at the opening of the SG and colocalised with the SG stem cell marker Blimp1. Further investigations showed that GPR39 was spatiotemporally expressed during skin wound repair. Although it was dispensable for skin development and homeostasis, GPR39 contributed positively to skin wound healing: its loss led to a delay in wound healing during the intermediate stage. The present study reveals a novel role of GPR39 in both dermatology and stem cell biology that has not been previously recognised.

G protein-coupled receptors (GPCRs) mediate multiple key biological processes in the body. As one of the most important groups of drug targets, GPCRs have been intensively studied in recent decades. In recent years, the roles of GPCRs as novel stem cell markers and in stem cell regulation have received attention. GPR39 is an orphan GPCR that is conserved across vertebrates[1]. It is expressed in a range of tissues and functions in a variety of physiological processes, such as insulin secretion[2,3], synaptic signalling[4] and gastric emptying[5]. The metabolic roles of GPR39 are well recognised, in strong contrast to the lack of knowledge about its functions in stem cell biology. However, several reports have implied its involvement in stem cell biology. GPR39 is upregulated in both normal human foetal kidney and stem-like Wilms' tumour xenografts[6,7]. It has also been reported to be a signature gene in human synovium–derived mesenchymal stem cells (MSCs)[8].

The mammalian skin epidermis comprises the stratified epithelium and its appendages including the hair follicle (HF), the sweat gland and the sebaceous gland (SG). Various populations of stem cells have been identified in different regions of the epidermis; they maintain homeostasis and the renewal of the entire skin epithelium, as well as play critical roles in skin repair after injuries. SG is an epidermal appendage that is important in skin barrier function and is involved in common skin diseases, such as acne vulgaris and androgenic alopecia[9]. An SG is usually intimately attached to an HF, forming a pilosebaceous unit[10]. Recent investigations have elucidated SG cellular dynamics during morphogenesis and homeostasis[11]. Importantly, stem cells of the SG have been identified, with the specific expression of the transcription factor Blimp1[12]. However, SG stem cells have been investigated less thoroughly than other stem cell populations in the HF, largely because of a lack of specific cell surface markers.

Using a reporter mouse model in which GPR39 expression was monitored by LacZ staining, we serendipitously discovered that in murine skin, GPR39 was uniquely expressed in SGs and colocalised with SG stem cells. Furthermore, using a skin wound model, we revealed intriguing spatiotemporal expression dynamics of GPR39 at the wound site and the positive involvement of GPR39 in the wound healing process.

Results

Unique promoter activity and mRNA expression of *Gpr39* in SGs. Using a previously described mouse model in which targeted insertion of the *lacZ* reporter gene disrupted the *Gpr39* locus, we monitored the expression of *Gpr39* by staining with X-gal. As shown in Fig. 1a, LacZ staining of the tail skin in 20-day-old $Gpr39^{+/lacZ}$ mice indicated specific *Gpr39* promoter activity at the openings of SGs (Fig. 1a, top). $Gpr39^{+/+}$ skin from negative-control littermate mice showed no such staining (Fig. 1a, bottom). In a separated hair follicle, $lacZ^{+}$ cell clusters were surrounded by sebocytes positive for Oil-Red-O (ORO) (Fig. 1b, left panel). After these sebocytes had been removed, the $lacZ^{+}$ cell cluster was clearly observed attached to the isthmus of the HF (Fig. 1b, right panel). We performed RT-PCR to examine the mRNA expression of *Gpr39* in various epidermal compartments. The separation of the epidermal compartments was verified by the expression of different markers in their corresponding compartments (Fig. S1). As indicated in Fig. 1c, *Gpr39* expression was detected in the pilosebaceous unit rather than in the interfollicular epidermis (IFE) (Fig. 1c). RNA *in situ* hybridisation also confirmed the existence of *Gpr39* mRNA within the SG opening (Fig. 1d). *lacZ* signals were also detected in the dorsal skin and exhibited a temporal upregulation around postnatal Day 24, when hair follicles entered a new anagen phase (Fig. 1e), indicating the cellular dynamics of *Gpr39* expression during the hair cycle.

$GPR39^{+}$ cells colocalise with $Blimp1^{+}$ SG stem cells. GPR39 protein expression in wild-type mice was examined by immunofluorescence staining. As shown in Fig. 2a, the membrane location of GPR39 was clear in the cells at the SG opening, where unipotent $Blimp1^{+}$ SG stem cells have been reported to reside[9]. To analyse the relationship between the $GPR39^{+}$ cells and the $Blimp1^{+}$ cells, we costained with these markers and found that GPR39 and Blimp1 largely marked the same cell population within the SG (Fig. 2b). GPR39 expression was also compared to the expression of the isthmus stem cell marker Lrig1. Whereas Lrig1 staining exhibited a typical isthmus distribution, $GPR39^{+}$ cells were observed adjacent to $Lrig1^{+}$ cells, with partial overlapping (Fig. 2c). After dispase digestion, we stained GPR39 and Blimp1 in detached SGs (Fig. 2d). These results also verified that GPR39 was expressed in small cells at the SG opening (Fig. 2e) and colocalised with Blimp1 (Fig. 2f). A flow cytometric analysis indicated that the $GPR39^{+}$ cells accounted for approximately 0.05% of all epidermal cells (Fig. 2g). In human skin, GPR39 expression was also restricted to the opening of the SG (Fig. 2h). In summary, the cell-specific expression of GPR39 and its colocalisation with Blimp1 suggested that GPR39 may mark a population of putative SG stem cells.

$GPR39^{+}$ cells differentiate and generate ORO^{+} sebocytes *in vitro*. We also characterised $GPR39^{+}$ SG cells *in vitro*. Tail SGs from 7- to 8-week-old mice were cultured *in vitro*. On D0 of culture, the SGs were positive for ORO (Fig. S2b), whereas only the small cells at the SG opening were positive for GPR39 (Fig. S2c). On D2 of culture, the $GPR39^{+}$ cells proliferated and migrated outwards (Fig. S2f), whereas the ORO^{+} sebocytes remained as clusters (Fig. S2e). After transient trypsinisation, the ORO^{+} sebocytes detached from the culture dish, whereas the $GPR39^{+}$ cells remained attached (Fig. S2 g, h and i). On D5, ORO^{+} cells reappeared in the culture, whereas the $GPR39^{+}$ cell number had decreased sharply (Fig. S2 j, k and l), suggesting that the $GPR39^{+}$ cells had differentiated into ORO^{+} cells. This *in vitro* assay implied that $GPR39^{+}$ cells are progenitor-like cells that can differentiate into ORO^{+} sebocytes.

GPR39 shows dynamic spatiotemporal expression during skin wound healing. The expression pattern of GPR39 suggested that it might play a role in the skin. However, $Gpr39^{-/-}$ mice showed no

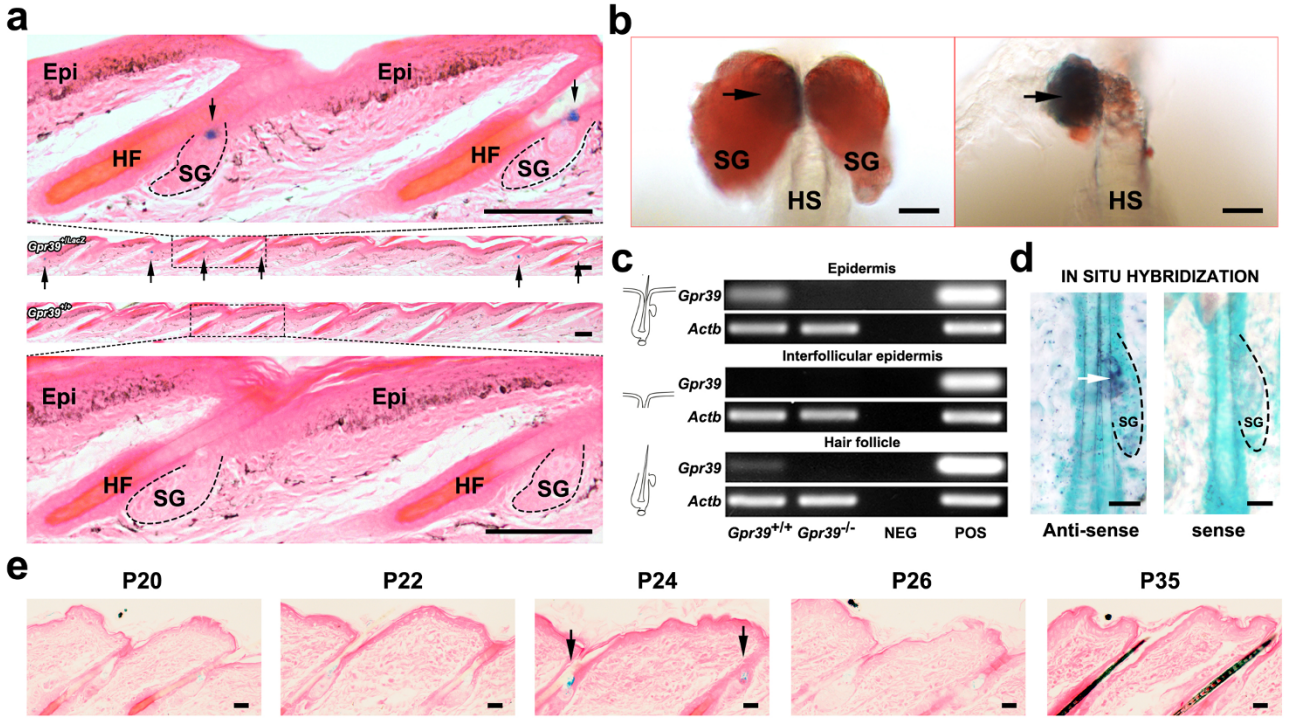

Figure 1 | Promoter activity and mRNA expression of *Gpr39* in the skin. (**a**) Microscopic observation of LacZ staining in tail skin of $Gpr39^{+/lacZ}$ (top) and $Gpr39^{+/+}$ (bottom) mice. Arrows indicate *lacZ* signals at the openings of SGs. (**b**) Whole-mount LacZ staining of an isolated intact hair follicle (HF) (left) and an HF with the sebocytes removed (right). The tissues were counter-stained with ORO. (**c**) RT-PCR examination of *Gpr39* and *Actb* (as an internal control) expression in separate epidermal compartments. NEG, negative control; POS, positive control. (**d**) RNA *in situ* hybridisation of *Gpr39* in the SG. (**e**) LacZ staining in the dorsal skin of $Gpr39^{+/lacZ}$ mice on different postnatal days. HF, hair follicle; SG, sebaceous gland; Epi, epidermis; HS, hair shaft; P20, postnatal Day 20. Bar (**a**) = 100 μm, (**b**) = 20 μm, (**d**) = 25 μm, (**e**) = 20 μm.

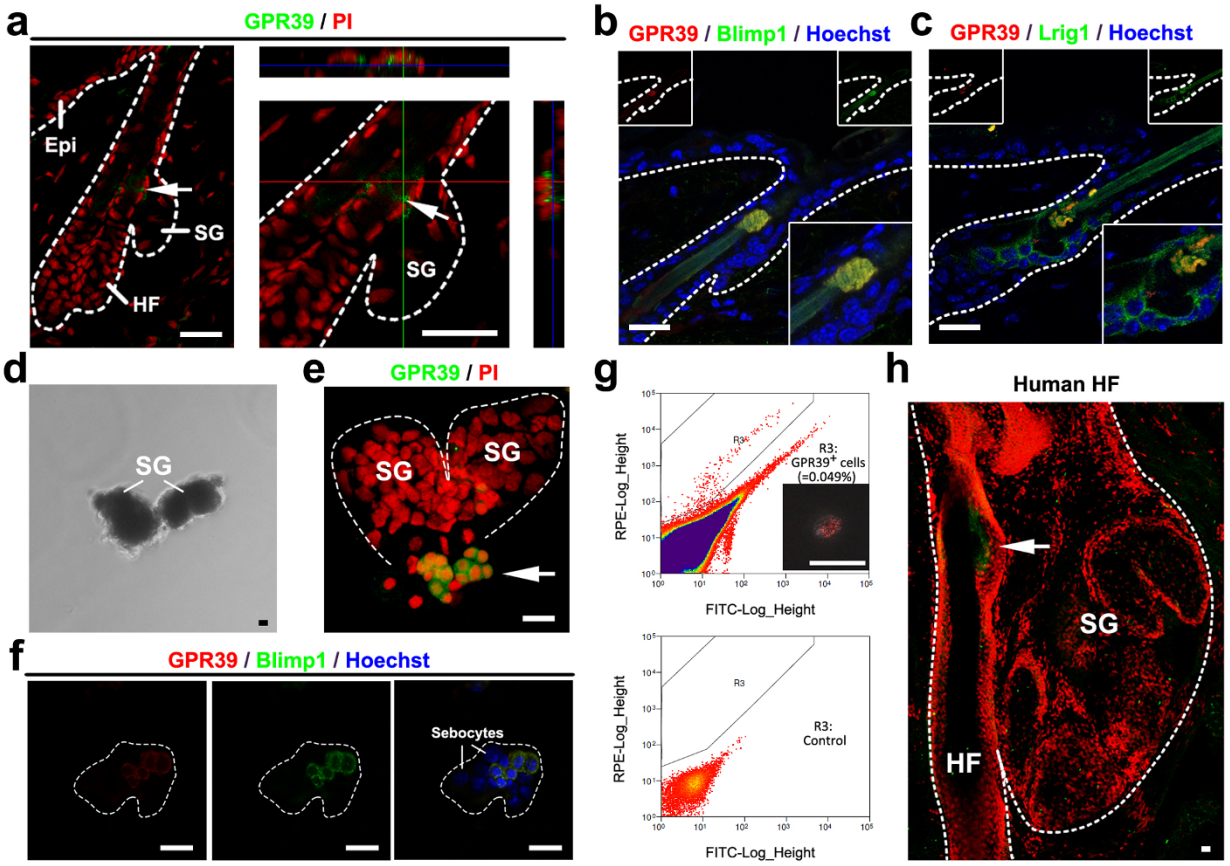

Figure 2 | Localisation of GPR39 protein expression in HFs. (**a**) Immunostaining of GPR39 (green) in the HF and SG. PI was used for counterstaining (red). (**b**) Costaining of GPR39 (red) and Blimp1 (green) in the HF. Hoechst was used for counterstaining (blue). Inserted in the panel are separate colour channels and an enlarged picture of the SG section. (**c**) Costaining of GPR39 (red) and Lrig1 (green) in the HF. (**d**) SGs detached from the tail skin after dispase digestion. (**e**) Immunostaining of GPR39 in detached SGs. PI was used for counter staining (red). (**f**) Costaining of GPR39 (red) and Blimp1 (green) in a detached SG. The cells were counterstained with Hoechst (blue). (**g**) Flow cytometric analysis of epidermal cells using a PE-conjugated GPR39 antibody. The upper panel shows cells stained with the GPR39 antibody, and the lower panel shows the negative control without antibody staining. Inserted in the upper panel is an image of a sorted cell with PE fluorescence. (**h**) Expression of GPR39 in a human hair follicle. Arrows indicate positive signals. HF, hair follicle; SG, sebaceous gland; Epi, epidermis. Bar (**a**) = 25 μm, (**b**, **c**) = 20 μm, (**d**) = 5 μm, (**e**, **f**, **g**, **h**) = 20 μm.

obvious defects in skin development or homeostasis. Therefore, we created a skin wound environment to further explore the function of GPR39. After making 1/8-inch, circular, full-thickness cutaneous wounds in the backs of *Gpr39*$^{+/lacZ}$ mice (7- to 8-week-old), we noted that GPR39 had intriguing expression dynamics in the wound area. On D2 after wounding, *lacZ* signals were barely detected in the epidermis (Fig. 3 a, b; first column). However, by D4, *lacZ* signals became evident in the epidermis at the edge of the wound (Fig. 3 a, b; second column). Along with the healing, the epidermal *lacZ* signals became restricted to the area within the wound on D6 (Fig. 3 a, b; third column). Upon wound closure, LacZ staining in the epidermis had decreased (Fig. 3 a, b; last column). The expression of the GPR39 protein in the wounded epidermis from D2 to D8 was also confirmed by immunostaining (Fig. 3c).

GPR39-deficient mice show a delay in skin wound repair during the intermediate stage. The intriguing expression pattern of GPR39 at the wound site implied a function of GPR39 in wound repair. To assess whether GPR39 was involved in skin wound repair, we made uniform skin wounds (1/8-inch, circular, full-thickness cutaneous wounds) in 7- to 8-week-old *Gpr39*$^{+/+}$ mice and in *Gpr39*$^{-/-}$ mice in which both *Gpr39* alleles had been replaced by *lacZ* sequences. We monitored and measured the wound size from D0 to D12 post wounding. Wound closure was slower in the *Gpr39*$^{-/-}$ mice than in their wild-type siblings (Fig. 4a). A statistical analysis of wound size change also indicated a significant delay in the wound closure rate in the *Gpr39*$^{-/-}$ mice on D6 and D8 (Fig. 4b), indicating that GPR39 contributes to skin wound healing.

Discussion

Although the *Gpr39* gene was cloned in 1997[13], research on its biological function has only emerged over the last 10 years. The vast majority of studies on this newly discovered orphan receptor have focused on its functions in metabolism. Our data on GPR39 expression in mouse skin suggest that GPR39 is a novel surface marker of putative SG stem cells. We also demonstrated that GPR39 is involved in skin wound repair. To our knowledge, the present study is the first report to examine GPR39 in skin tissue.

Several studies had reported the expression of GPR39 in cell populations with stem/progenitor cell properties. Microarray data have indicated the upregulation of *Gpr39* expression in stem-like Wilms' tumour xenografts, which are highly rich in progenitor cells[6,7]. In chondrogenic human synovium-derived MSCs, the CpG-rich region of the *Gpr39* gene promoter was shown to be hypomethylated, and *Gpr39* expression was found to be downregulated upon differentiation towards chondrocytes[8]. Here, using different methods, we clearly demonstrated the expression of GPR39 at the openings of SGs, at the exact position where SG stem cells reside. The colocalisation of GPR39 and the SG stem cell marker Blimp1 in the same cell population and the presence of GPR39^{+} cells adjacent to Lrig1^{+}

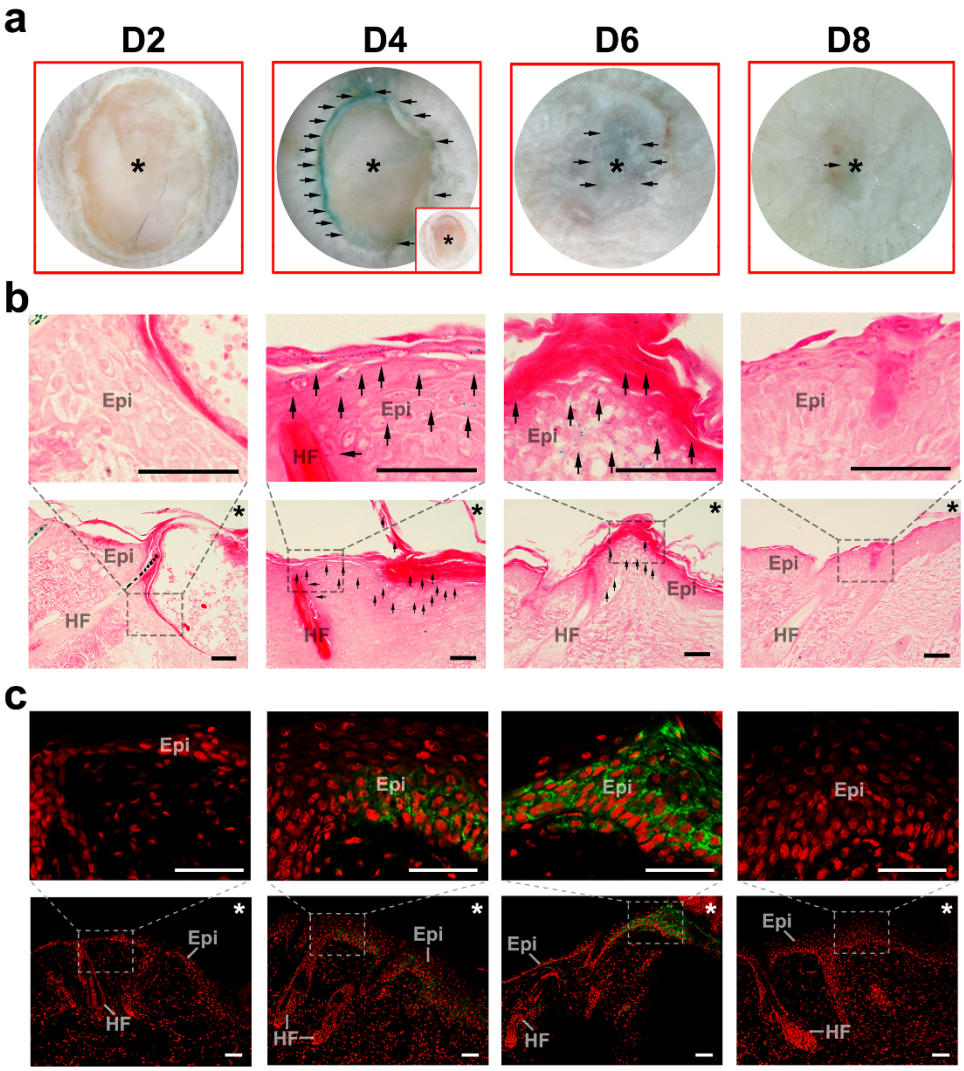

Figure 3 | Expression dynamics of GPR39 after wounding. (**a**) Whole-mount LacZ staining in wounded skin of *Gpr39*$^{+/lacZ}$ mice on different days after wounding. Inserted in the D4 image is a negative control showing no LacZ staining in *Gpr39*$^{+/+}$ mice. (**b**) Microscopic observation of *lacZ* expression in wounded skin of *Gpr39*$^{+/lacZ}$ mice on different days after wounding. The upper panels are magnifications of the framed areas in the lower panels. (**c**) GPR39 immunostaining on D2, 4, 6 and 8 after wounding. The upper panels are magnifications of the framed areas in the lower panels. Black arrows indicate *lacZ*$^{+}$ cells. Asterisks indicate the wound site. Epi, epidermis; HF, hair follicle. Bar = 50 μm.

isthmus stem cells further supported GPR39 as a putative signature gene for SG stem cells. Unfortunately, the limited number of GPR39^{+} SG cells and our inability to culture them *in vitro* made it difficult to fully characterise these cells. However, our preliminary *in vitro* data support the notion that GPR39^{+} SG cells can differentiate into sebocytes. Interestingly, the expression of GPR39 in SGs in dorsal skin was phase dependent, whereas it was robust in most of the tail SGs. The possible explanation is that tail SGs are more well-developed than dorsal SGs and tail skin has less drastic morphological change during the hair cycle progression compared with dorsal skin. Despite its abundant expression in putative SG stem cells, GPR39 seemed to function only as a marker, rather than as an important regulator: *Gpr39*$^{-/-}$ SGs or epidermis showed no obvious differences from their wild-type counterparts. Intriguingly, several other GPCRs have recently been identified as definitive markers for different stem/progenitor cell populations within the HF, and for epithelial stem cells in other tissues. These GPCRs include the highly concerned leucine-rich repeat-containing GPCRs, LGR4/5/6[14–16].

GPR39 was previously found to be involved in cell migration and epithelial repair *in vitro* in HaCaT cells, an immortalised human keratinocyte cell line[17]. Here, we discovered the role of GPR39 in skin wound healing *in vivo*. Skin wound healing is a complex biological process involving changes in the epidermis, dermis and vasculature; it is characterised by three continuous, overlapping phases: an inflammatory phase, a proliferative phase and a contraction and remodelling phase[18]. The proliferative phase further contains two interdependent stages: an initial keratinocyte-mediated stage, in which epidermal cells proliferate and migrate to seal the epithelial barrier, followed by a fibroblast-mediated phase, in which the dermis is remodelled[19]. Given that GPR39 expression was found only in SGs and wounded epidermis, we consider that the function of GPR39 is also restricted to the epidermis. Interestingly, GPR39 expression in the wounded epidermis was the highest during D4–6 after wounding, when the wounded epidermis exhibited a drastic increase in thickness. These data suggest that GPR39 might be associated with the proliferation and/or migration of epidermal cells during D4–6; as a consequence, GPR39-mutant mice showed significantly impaired wound closure later during D6–8. However because GPR39 was not involved in other events, such as dermal remodelling and contraction, its loss was not sufficient to devastate the entire wound healing process. It is why GPR39-mutant wounds finally closed during D13–14, which is also the case for many other defects[18,20].

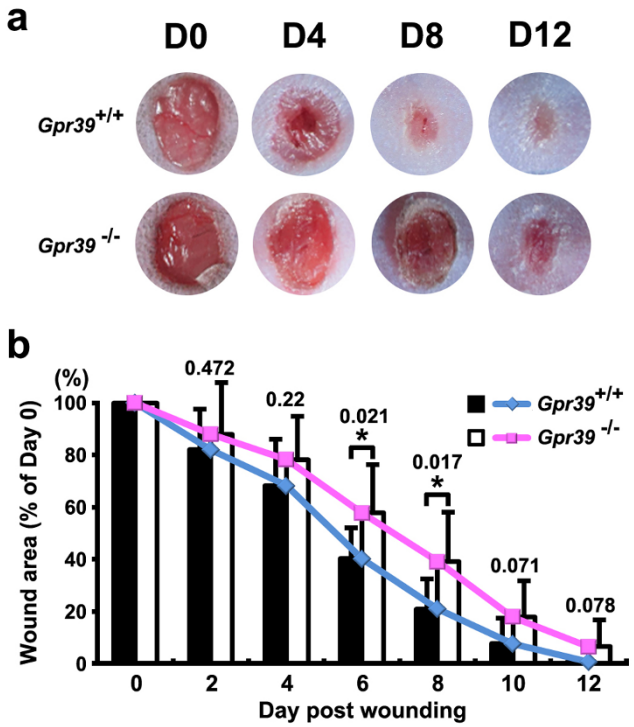

Figure 4 | Wound healing assay in *Gpr39*$^{+/+}$ and *Gpr39*$^{-/-}$ mice. (**a**) Images of wound areas in *Gpr39*$^{+/+}$ and *Gpr39*$^{-/-}$ mice on different days after wounding, with the same magnification. (**b**) Statistical analysis of wound size change in both *Gpr39*$^{+/+}$ and *Gpr39*$^{-/-}$ mice. The *P* value for each comparison is labelled above the columns. The data present the means ± SEM, and the asterisks indicate statistically significant differences with a P value < 0.05.

Epidermal regeneration after wounding involves the contributions of various stem/progenitor cell populations, depending on the circumstances, although normal epidermal homeostasis is dependent on distinct stem cell populations replacing local dead cells[21]. The progeny of HFSCs in the bulge and the upper follicle have been reported to migrate out to repair the IFE[14,15,22,23], whereas IFE stem cells alone are also able to repair cutaneous wounds[24]. Even unipotent stem cells in sweat glands can migrate upwards to repair the damaged epidermis[25]. There is currently no evidence showing that SG stem cells can contribute to epidermal wound repair. As to the present study, it is of great interest to determine whether the SG cells that expressed GPR39 migrated out to the injured epidermis to exert their functions or the presence of GPR39^{+} cells at the wound site was caused by *de novo* GPR39 expression. Additional animal models are needed to lineage-trace GPR39^{+} SG cells and their progeny to unambiguously address these different possibilities.

Although the cognate ligand for GPR39 has not yet been definitively determined, several studies have provided some clues about GPR39 signalling. As a member of the ghrelin receptor family, GPR39 has constitutive activity mainly through the serum response element-dependent pathway[26]. It has been reported that Zn^{2+} binds to and activates GPR39[1,27,28]. In HaCaT cells, GPR39-mediated epithelial repair was also triggered by Zn^{2+} released from injured cells[17]. Recent research revealed that GPR39 is a regulator of the Hedgehog pathway[29]. The Hedgehog pathway, mainly the Sonic Hedgehog (Shh) pathway, is involved in multiple stages of skin morphogenesis and may have the ability to modulate several aspects of wound healing[30,31]. The Hedgehog pathway is also known to play a key role in regulating SG development[32] and the proliferation of SG progenitors[33]. It is possible that the roles of GPR39 in SGs and epidermal wound repair are associated with the Hedgehog pathway. Nevertheless, to fully dissect the mechanism of GPR39 function in the skin requires exploration of its ligand and intracellular signal transduction.

In summary, our pioneering work exposed a novel role for GPR39 in SGs and epidermal wound repair. Given the importance of GPCRs as cellular drug targets, further comprehensive investigations into GPR39 under skin wounding and pathological conditions might shed light on treatments for cutaneous wound repair and skin disorders such as acne vulgaris.

Methods

Mice. Mouse husbandry, breeding and use were performed according to the "Guidelines for the Care and Use of Animals in Research" of the Institute of Zoology, Chinese Academy of Sciences. All of the mice were maintained under specific-pathogen-free (SPF) conditions with a constant photoperiod (12L : 12D) and free access to water and food. All of the experiments involving the use of laboratory mice were approved by the ethics committee of the Institute of Zoology, Chinese Academy of Sciences.

Heterozygous mice (*Gpr39*$^{+/lacZ}$) were generated as previously described by Lexicon Genetics, Inc. (Woodlands, TX)[34]. In these mice, the targeted insertion of the *lacZ* reporter gene disrupted the *Gpr39* locus, leading to the replacement of endogenous *Gpr39* expression by *lacZ* expression. Thus, homozygous mutants (*Gpr39*$^{lacZ/lacZ}$) were GPR39 knockouts (*Gpr39*$^{-/-}$). For mouse genotyping, the primers 5′-ACCCTCATCTTGGTGTACCT-3′ and 5′-ATGTAGCGCTCAAAGCTGAG-3′ were used to amplify the wild-type-specific band, whereas the primers 5′-GGAACTCTCACTCGACCTGGG-3′ and 5′-GCAGCGCATCGCCTTCTATC-3′ were used to amplify the mutation-specific band.

β-galactosidase (LacZ) staining and Oil-Red-O (ORO) counterstaining. Epidermal sheets and skin tissues were isolated at the indicated time points from *Gpr39*$^{+/lacZ}$ and *Gpr39*$^{+/+}$ mice. Whole tissues were fixed in a 4% paraformaldehyde (PFA) solution (containing 0.1 mol/L PIPES buffer [pH 6.9], 2 mM $MgCl_2$, and 5 mM EGTA) (Sigma) for 30 minutes at 4°C. The fixed tissues were rinsed in phosphate-buffered saline (PBS, containing 2 mM $MgCl_2$, 0.01% sodium deoxycholate and 0.02% NP-40) three times at room temperature for 30 minutes and were then incubated in staining solution (containing 0.1 M phosphate buffer, 2 mM $MgCl_2$, 0.01% sodium deoxycholate, 0.02% NP-40, 5 mM potassium ferricyanide, 5 mM potassium ferrocyanide and 1 mg/mL X-Gal) (Sigma) overnight at 37°C. Alcohol (70%) was used to stop the reaction and store the tissues.

To accurately localise *lacZ* expression in the SGs, some epidermal sheets were counterstained with ORO (Sigma). After being pre-incubated in 60% isopropanol for 5 minutes, tissue samples were counterstained in an ORO staining solution containing 0.5% ORO in a mixture of propanol and distilled water at a volume ratio of 3 : 2. The SGs were clearly observed within 5 minutes because of ORO absorption. The tissue samples were washed with 60% isopropanol to remove any remaining staining solution and were stored in PBS.

For more detailed histological observations, whole-mount-stained tissues were dehydrated with gradient alcohol and were embedded in paraffin. Sections were cut at a thickness of 20 μm. After being deparaffinised and rehydrated, the tissue sections were counterstained with eosin.

RNA extraction and RT-PCR. Different regions of the mouse tail epidermis were dissected for RNA extraction and RT-PCR, as indicated in Fig. 1c. The entire epidermal sheet (with hair follicles) was peeled off from the dermis after an overnight incubation with dispase (1 mg/mL, Gibco) at 4°C. The hair follicles were subsequently dissected from the epidermal sheet with 0.1 mm forceps, with the remaining tissue being the IFE.

The RNeasy Micro Kit (Qiagen) was used to extract total RNA from the separate epidermal regions described above. cDNA was generated with M-MuLV reverse transcriptase (New England Biolabs). PCR was performed using Promega PCR Master Mix. The PCR cycle for *Actb* (*β-actin*) or other genes was as follows: 95°C for 4 minutes; 23 or 30 cycles of 95°C for 30 seconds, 57°C or 60°C for 30 seconds and 72°C for 30 seconds; and 72°C for 5 minutes. The primers used to amplify different genes were listed in Table S1. *Actb* was used as an internal control.

RNA *in situ* hybridisation (ISH). *In situ* hybridization with digoxygenin-labeled antisense RNA probes was performed on frozen sections as previously described[35]. The primers used to generate the antisense probes were 5′–GTGGTCCTGGCGTC-TGTGGC-3′ and 5′-GGGCACGCTGGCGTTTCTCT-3′. The sense probes were used as the negative control.

Immunofluorescence staining. Frozen sections (20 μm thick) were fixed in 4% PFA/PBS for 10 minutes at room temperature. After being penetrated with 0.5% Triton for 10 minutes at room temperature, the sections were blocked in PBS containing 5% bovine serum albumin (BSA) or 5% rabbit serum for 1 hour in 37°C, followed by incubation with primary antibodies diluted in 1% BSA/PBS or 1% rabbit serum at 4°C in a humid chamber. After being washed with PBS three times, the sections were incubated with secondary antibodies diluted in 1% BSA/PBS or 1% rabbit serum for 1 hour in 37°C. Propidium iodide (PI, Sigma) or Hoechst33342 (Sigma) was used to

label the nuclei. The sections were mounted and photographed under a confocal microscope (ZEISS).

The primary antibodies were rabbit anti-GPR39 (NLS139, NOVUS), rabbit anti-GPR39 (NLS142, NOVUS), goat anti-Blimp1 (ab13700, Abcam) and goat anti-Lrig1 (AF3688, R&D Systems) antibodies. The secondary antibodies were purchased from ZSGB-BIO.

SG isolation and *in vitro* culture. After overnight dispase digestion (1 mg/mL in PBS) at 4°C, SGs from 7- to 8-week-old mice were easily detached from the tail epidermis. Intact SGs were subsequently fixed with 4% PFA/PBS for staining or were cultured in DMEM (Gibco) with 20% foetal bovine serum (FBS, Hyclone). SGs and SG outgrowth were transiently digested with 0.05% trypsin on D2 of culture to remove sebocytes. The cultures were fixed for ORO staining and GPR39 immunostaining on D0, D2 and D5.

Flow cytometry. The entire epidermal sheets (with hair follicles) from the backs of 7- to 8-week-old mice were peeled off from the dermis after dispase digestion and were further trypsinised into single cells and incubated with a PE-conjugated rabbit anti-GPR39 antibody (bs-5789R-PE, Bioss) diluted with 5% FBS in PBS. After serial washes, epidermal cells were analysed on a MoFlo flow cytometer.

***In vivo* wound healing assay and statistical analysis.** $Gpr39^{-/-}$ mice (n = 5) and their wild-type littermates (n = 5) at 7–8 weeks were used in the skin wound healing assay. Two 1/8-inch, circular, full-thickness cutaneous wounds were made with a punch (FISKARS) on the back of each mouse. The wounds were photographed on Days 0, 2, 4, 6, 8, 10, and 12 post-wounding. The wound area was calculated using NIH ImageJ software and was indicated as the percentage of the area on D0.

A statistical comparison of the wound areas between $Gpr39^{+/+}$ and $Gpr39^{-/-}$ mice was performed using Student's *t*-test (two-tailed), and all the data are presented as the means ± SEM. Differences were considered significant when $P < 0.05$.

The same procedure was used to generate wounds on the backs of $Gpr3^{+/lacZ}$ mice. Wounded tissue and the surrounding healthy skin was collected for histological analysis on different days after injury. The collected skin samples were stored at -80°C for cryosectioning or were fixed in 4% PFA solution for LacZ staining.

1. Popovics, P. & Stewart, A. J. GPR39: a Zn(2+)-activated G protein-coupled receptor that regulates pancreatic, gastrointestinal and neuronal functions. *Cell Mol. Life Sci.* **68**, 85–95 (2011).
2. Holst, B. *et al.* G protein-coupled receptor 39 deficiency is associated with pancreatic islet dysfunction. *Endocrinology* **150**, 2577–2585 (2009).
3. Tremblay, F. *et al.* Disruption of G protein-coupled receptor 39 impairs insulin secretion in vivo. *Endocrinology* **150**, 2586–2595 (2009).
4. Jackson, V. R., Nothacker, H. P. & Civelli, O. GPR39 receptor expression in the mouse brain. *Neuroreport* **17**, 813–816 (2006).
5. Egerod, K. L. *et al.* GPR39 splice variants versus antisense gene LYPD1: expression and regulation in gastrointestinal tract, endocrine pancreas, liver, and white adipose tissue. *Mol. Endocrinol.* **21**, 1685–1698 (2007).
6. Dekel, B. *et al.* Multiple imprinted and stemness genes provide a link between normal and tumor progenitor cells of the developing human kidney. *Cancer Res.* **66**, 6040–6049 (2006).
7. Metsuyanim, S. *et al.* Expression of stem cell markers in the human fetal kidney. *PLoS One* **4**, e6709 (2009).
8. Ezura, Y., Sekiya, I., Koga, H., Muneta, T. & Noda, M. Methylation status of CpG islands in the promoter regions of signature genes during chondrogenesis of human synovium-derived mesenchymal stem cells. *Arthritis Rheum.* **60**, 1416–1426 (2009).
9. Hinde, E. *et al.* A practical guide for the study of human and murine sebaceous glands in situ. *Exp. Dermatol.* **22**, 631–637 (2013).
10. Niemann, C. & Horsley, V. Development and homeostasis of the sebaceous gland. *Sem. Cell Dev. Biol.* **23**, 928–936 (2012).
11. Frances, D. & Niemann, C. Stem cell dynamics in sebaceous gland morphogenesis in mouse skin. *Dev. Biol.* **363**, 138–146 (2012).
12. Horsley, V. *et al.* Blimp1 defines a progenitor population that governs cellular input to the sebaceous gland. *Cell* **126**, 597–609 (2006).
13. McKee, K. K. *et al.* Cloning and characterization of two human G protein-coupled receptor genes (GPR38 and GPR39) related to the growth hormone secretagogue and neurotensin receptors. *Genomics* **46**, 426–434 (1997).
14. Jaks, V. *et al.* Lgr5 marks cycling, yet long-lived, hair follicle stem cells. *Nat. Genet.* **40**, 1291–1299 (2008).
15. Snippert, H. J. *et al.* Lgr6 marks stem cells in the hair follicle that generate all cell lineages of the skin. *Science* **327**, 1385–1389 (2010).
16. Barker, N., Tan, S. & Clevers, H. Lgr proteins in epithelial stem cell biology. *Development* **140**, 2484–2494 (2013).
17. Sharir, H., Zinger, A., Nevo, A., Sekler, I. & Hershfinkel, M. Zinc released from injured cells is acting via the Zn2+-sensing receptor, ZnR, to trigger signaling leading to epithelial repair. *J. Biol. Chem.* **285**, 26097–26106 (2010).
18. Hattori, N. *et al.* MMP-13 plays a role in keratinocyte migration, angiogenesis, and contraction in mouse skin wound healing. *Am. J. Pathol.* **175**, 533–546 (2009).
19. Schmidt, B. A. & Horsley, V. Intradermal adipocytes mediate fibroblast recruitment during skin wound healing. *Development* **140**, 1517–1527 (2013).
20. Kim, K-T. *et al.* High-power femtosecond-terahertz pulse induces a wound response in mouse skin. *Sci. Rep.* **3**, 2296 (2013).
21. Blanpain, C. & Fuchs, E. Stem cell plasticity. Plasticity of epithelial stem cells in tissue regeneration. *Science* **344**, 1242281 (2014).
22. Ito, M. *et al.* Stem cells in the hair follicle bulge contribute to wound repair but not to homeostasis of the epidermis. *Nat. Med.* **11**, 1351–1354 (2005).
23. Levy, V., Lindon, C., Zheng, Y., Harfe, B. D. & Morgan, B. A. Epidermal stem cells arise from the hair follicle after wounding. *FASEB J.* **21**, 1358–1366 (2007).
24. Langton, A. K., Herrick, S. E. & Headon, D. J. An extended epidermal response heals cutaneous wounds in the absence of a hair follicle stem cell contribution. *J. Invest. Dermatol.* **128**, 1311–1318 (2008).
25. Lu, C. P. *et al.* Identification of stem cell populations in sweat glands and ducts reveals roles in homeostasis and wound repair. *Cell* **150**, 136–150 (2012).
26. Holst, B. *et al.* Common structural basis for constitutive activity of the ghrelin receptor family. *J. Biol. Chem.* **279**, 53806–53817 (2004).
27. Holst, B. *et al.* GPR39 signaling is stimulated by zinc ions but not by obestatin. *Endocrinology* **148**, 13–20 (2007).
28. Lauwers, E., Landuyt, B., Arckens, L., Schoofs, L. & Luyten, W. Obestatin does not activate orphan G protein-coupled receptor GPR39. *Biochem. Biophys. Res. Commun.* **351**, 21–25 (2006).
29. Bassilana, F. *et al.* Target identification for a Hedgehog pathway inhibitor reveals the receptor GPR39. *Nat. Chem. Biol.* **10**, 343–349 (2014).
30. Le, H. *et al.* Hedgehog signaling is essential for normal wound healing. *Wound Repair Regen.* **16**, 768–773 (2008).
31. Luo, J. *et al.* Sonic hedgehog improves delayed wound healing via enhancing cutaneous nitric oxide function in diabetes. *Am. J. Physiol.-Endoc. M.* **297**, e525–e531 (2009).
32. Allen, M. *et al.* Hedgehog Signaling Regulates Sebaceous Gland Development. *Am. J. Pathol.* **163**, 2173–2178 (2003).
33. Niemann, C. *et al.* Indian hedgehog and beta-catenin signaling: role in the sebaceous lineage of normal and neoplastic mammalian epidermis. *Proc. Natl. Acad. Sci. U S A* **100 Suppl 1**, 11873–11880 (2003).
34. Moechars, D. *et al.* Altered gastrointestinal and metabolic function in the GPR39-obestatin receptor-knockout mouse. *Gastroenterology* **131**, 1131–1141 (2006).
35. Kuang, H. *et al.* CXCL14 inhibits trophoblast outgrowth via a paracrine/autocrine manner during early pregnancy in mice. *J. Cell Physiol.* **221**, 448–457 (2009).

Acknowledgments

We thank members of the Duan laboratory for comments and suggestions. We thank Ms. Tong Zhao at the Institute of Microbiology, Chinese Academy of Sciences for her kind help with flow cytometric experiments. This work was supported by the Strategic Priority Research Program of the Chinese Academy of Sciences XDA 01010202 (to E. Duan), the National Basic Research Program of China 2011CB710905 (to E. DUAN), and the National Natural Science Foundation of China 31201099 (to S. Liu).

Author contributions

H.S. Zhao, S.L. and E.K.D. conceived and designed the experiments; H.S. Zhao, J.Q.Q., H.S. Zhang, X.Y.W. and Z.L.D. performed the experiments; H.S. Zhao, S.B.Z., X.H.L. and Y.G. analysed the data; L.N.N., Y.J.C. and Y.G. contributed reagents/materials/analysis tools; and H.S. Zhao, S.L. and E.K.D. wrote the manuscript.

Additional information

Supplementary information accompanies this paper at http://www.nature.com/scientificreports

Competing financial interests: The authors declare no competing financial interests.

How to cite this article: Zhao, H. *et al.* GPR39 marks specific cells within the sebaceous gland and contributes to skin wound healing. *Sci. Rep.* **5**, 7913; DOI:10.1038/srep07913 (2015).